

SUPPORTING INFORMATION

Predicting Self-Assembly: From Empirism to Determinism

Carlos-Andres Palma, Marco Cecchini*, and Paolo Samorì*

*ISIS/UMR CNRS 7006, Université de Strasbourg
8, allée Gaspard Monge, 67000 Strasbourg, France*

Entropy and Partition Function

Eq. 5 in the *Main Text* reads

$$S = \frac{\partial(kT \ln Z)}{\partial T} \quad (1)$$

if the energy levels accessible to the system are similar one another, i.e. $E_j \rightarrow \text{const}$, the system partition function becomes

$$Z = \sum_i^M e^{-\beta C} = M e^{-\beta C} \quad (2)$$

with $\beta = \frac{1}{kT}$ and M the number of accessible states at given thermodynamic conditions. By rearranging Eq. 2 as

$$\begin{aligned} \ln Z &= \ln M - \beta C \\ kT \ln Z &= kT \ln M - C \end{aligned}$$

one obtains

$$\frac{\partial(kT \ln Z)}{\partial T} = k \ln M \quad (3)$$

that is Eq. 6 in the *Main Text*. Interestingly, Eq. 3 states that if $E_j \rightarrow \text{const}$, entropy can be written in a closed form which depends logarithmically on the total number of accessible states, M . Importantly, this result shows that S converges very slowly with M such that its value can be analytically evaluated for none but the simplest systems (see *Main Text*).

Molecular self-assembly from thermal to chemical equilibrium

Given a closed system in which the following chemical transformation $\alpha a \rightleftharpoons \beta b$ takes place, its absolute free energy depends on the temperature T , volume V , and chemical composition

$$F = F(V, T, n_a, n_b) \quad (4)$$

where n_a and n_b are, respectively, the number of moles of a and b in the given volume. From Eq. 48 it follows that

$$dF = -p dV - S dT + \mu_a dn_a + \mu_b dn_b \quad (5)$$

where

$$\mu_i = \left(\frac{\partial F}{\partial n_i} \right)_{T, V, n_j} \quad (6)$$

is called the chemical potential of the i -th specie. At constant temperature and volume, Eq. 5 yields

$$dF = \mu_a dn_a + \mu_b dn_b \quad (7)$$

which shows that an infinitesimal variation in the system's chemical composition corresponds to a change in free energy that depends on the chemical potentials of the species involved. Therefore, if one introduces the extent of reaction variable ξ , such that

$$\begin{aligned} dn_a &= -\alpha d\xi \\ dn_b &= \beta d\xi \end{aligned} \quad (8)$$

where the minus sign is used for consumption and the plus sign for production, and $d\xi = dn$, because ξ describes the amount of matter that is chemically transformed, Eq. 7 can be usefully rewritten as

$$\left(\frac{dF}{dn} \right)_{V, T} = \beta \mu_b - \alpha \mu_a = \Delta \mu_{b,a} \quad (9)$$

which makes the link between the system's free energy and the difference in the chemical potential of the species involved. At chemical equilibrium $dF = 0$, i.e. the system's free energy lies in a minimum, and Eq. 9 yields

$$\Delta \mu_{b,a} = \beta \mu_b - \alpha \mu_a = 0 \quad (10)$$

which states that chemical equilibrium implies the equality of the chemical potentials multiplied by their stoichiometric coefficients as $\beta\mu_b = \alpha\mu_a$. The latter provides a general thermodynamic condition for chemical equilibrium, i.e. $\sum_i \nu_i \mu_i = 0$.

The statistical mechanics expression of the chemical potential of the i -th specie

$$\mu_i = -kT \left(\frac{\partial \ln Z}{\partial n_i} \right)_{T,V,n_j} \quad (11)$$

provides the link between the concepts of thermal and chemical equilibrium. If we now assume that the chemical species are independent and distinguishable [1], i.e. a mixture of ideal gases or a highly diluted solution, the system's partition function can be written as the product of the partition functions of the individual components as

$$Z(V, T, n_a, n_b) = Z(V, T, n_a) Z(V, T, n_b) \quad (12)$$

In addition, if particles of a chemical species are considered as independent and indistinguishable the canonical partition function can be expressed in terms of *molecular partition functions*, z_i , and Eq.12 becomes

$$Z(V, T, n_a, n_b) = \frac{z_a(V, T)^{n_a}}{n_a!} \frac{z_b(V, T)^{n_b}}{n_b!} \quad (13)$$

By introducing the result of Eq. 13 into Eq. 11 one obtains expressions for the chemical potentials in terms of molecular partition functions

$$\mu_i = -kT \ln \frac{z_i(V, T)}{n_i} \quad (14)$$

where Stirling's approximation has been used for $n_i!$ Note that the latter is an asymptotic approximation that holds only when n is large; it follows that the equivalence of molecular partition functions and molecules, which we are going to derive, holds only within this boundary. Eq.14 states that under the previous assumptions (i.e independence of chemical species and particles) the chemical potential of one species can be determined as if the others were not present. Importantly, this result allows to move from the thermal equilibrium interpretation of self-assembly (Fig. 1 in *Main Text*) to chemical equilibrium (Fig. 4 in *Main Text*), which opens the way to a molecular interpretation of self-assembly. By integrating Eq. 9

$$\Delta\mu_{b,a} = \beta \left(-kT \ln \frac{z_b}{n_b} \right) - \alpha \left(-kT \ln \frac{z_a}{n_a} \right) \quad (15)$$

and rearranging the result, one can express the difference in chemical potential between the self-assembled state (**b**) and the melt (**a**) as

$$\Delta\mu_{b,a} = -kT \ln \left[\left(\frac{z_b}{n_b} \right)^\beta \left(\frac{n_a}{z_a} \right)^\alpha \right] = -kT \ln \frac{z_b^\beta}{z_a^\alpha} + kT \ln \frac{n_b^\beta}{n_a^\alpha} \quad (16)$$

where the first term of the rhs of Eq. 16 depends on the molecular partition functions only and is a (chemical) equilibrium contribution, while the second term depends on the actual concentrations of the chemical species involved and can be considered as an out-of-chemical-equilibrium correction to the difference in free energy per molecule. Thus, Eq. 16 can be rewritten as

$$\Delta\mu_{b,a} = \Delta\mu_{b,a}^{\circ} - \Delta\mu'_{b,a} \quad (17)$$

where the signs $^{\circ}$ and $'$ indicate chemical equilibrium and out-of-chemical-equilibrium conditions, respectively. Finally, at chemical equilibrium (see Eq. 10) the latter yields

$$\Delta\mu_{b,a}^{\circ} = -kT \ln \left(\frac{z_b^{\beta}}{z_a^{\alpha}} \right) = -kT \ln \left(\frac{n_b^{\beta}}{n_a^{\alpha}} \right)_{V,T}^{\circ} = kT \ln K_{\text{eq}} \Big|_{V,T} \quad (18)$$

that is the equilibrium result of Eq. 13 in the *Main Text*. We note that Eq. 18 implies the equivalence of molecular partition functions and number of molecules at chemical equilibrium, i.e. $z_b^{\beta}/z_a^{\alpha} = (n_b^{\beta}/n_a^{\alpha})^{\circ}$, which provides a straightforward interpretation of Eq. 16. In fact, introducing this equivalence and rearranging Eq. 16 gives

$$\Delta\mu_{b,a} = -kT \ln \left(\frac{n_b^{\circ}}{n_b} \right)^{\beta} - kT \ln \left(\frac{n_a}{n_a^{\circ}} \right)^{\alpha} \quad (19)$$

By comparing Eqs. 16 and 18, it appears that at constant temperature and volume the out-of-chemical-equilibrium character of self-assembly uniquely arises from the difference in composition between the initial and equilibrium conditions, i.e. $n_i \neq n_i^{\circ}$. Eq. 19 captures this aspect and provides a general and insightful description of self-assembly in terms of molecular concentrations at any initial conditions. In fact, for a molecular system in which the self-assembled state (**b**) and the melt (**a**) are in equilibrium experience suggests that a sudden increase in the concentration of molecules in the monomeric state (i.e. addition of an aliquot of **a**) will result in a free energy gradient towards assembly and a new equilibrium state. Here, we show how Eq. 19 may account for this. In fact, when fresh monomers are introduced into the system, the concentration of molecules in the **a** state will suddenly increase such that $n_a > n_a^{\circ}$, while $n_b = n_b^{\circ}$. It follows that n_a/n_a° will be larger than the unity and its logarithm will be positive. Thus, the first term of the r.h.s. of Eq. 19 will be zero and the second term negative, which yields $\Delta\mu_{b,a} < 0$ and $\Delta\mu'_{b,a} < \Delta\mu_{b,a}^{\circ}$. Given that $\mu_b^{\circ} = \mu'_b$, the latter implies $\mu'_a > \mu_a^{\circ}$. Hence, Eq. 19 predicts that a sudden increase in the concentration of the melt will result in an increased chemical potential of **a** (or equivalently an increase in the effective free energy per molecule) that gives rise to the mentioned free-energy gradient; see Fig. S1.

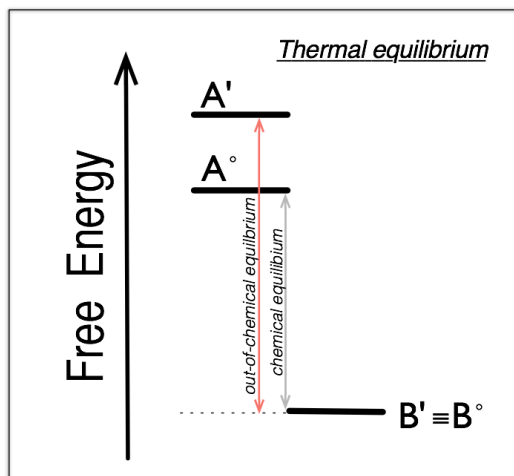


FIG. S1: Thermodynamics of self-assembly at thermal equilibrium. The figure provides a pictorial representation of the interpretation of chemical equilibrium grasped by Eq. 16. The signs $^{\circ}$ and $'$ indicate, respectively, chemical equilibrium and out-of-chemical-equilibrium conditions.

Critical Aggregate Concentration

Eq. 18 of *Main Text* reads

$$N_b = mN_a^m e^{-m\beta\Delta\mu_{b,a}^{\circ}} \quad (20)$$

with m the stoichiometric coefficient of the assembly reaction, $ma \rightleftharpoons b$, N_a and N_b the number of building blocks respectively populating the disassembled and the assembled state, and $\Delta\mu_{b,a}^{\circ}$ the free energy change of transferring one molecule from the monomeric to the self-assembled phase at standard chemical equilibrium conditions; here $\beta = \frac{1}{kT}$. As N_b cannot increase beyond N_{init} , otherwise it violates the mass balance, Eq. 20 gives

$$N_a \leq \left(\frac{N_{\text{init}}}{m} \right)^{\frac{1}{m}} e^{\beta\Delta\mu_{b,a}^{\circ}} \quad (21)$$

For increasing values of m , i.e. larger and larger self-assembled architectures, $(\frac{N_{\text{init}}}{m})^{1/m}$ goes to one and Eq. 21 provides an expression for the so-called *critical aggregate concentration* (CAC)

$$(N_a)_{\text{CAC}} \approx e^{\beta\Delta\mu_{b,a}^{\circ}} \quad (22)$$

which predicts the concentration of monomers above which molecules start aggregating; see Eq. 19 of *Main Text*. This result, which happens to be quite useful, is exact for large values of m . The

proof for Eq. 22 follows. Observing that $x^{1/x} = e^{\ln x/x}$ (see note ¹), in fact, it follows that

$$\lim_{x \rightarrow \infty} x^{1/x} = \lim_{x \rightarrow \infty} e^{\ln x/x} = 1, \quad (23)$$

Given that

$$\lim_{x \rightarrow \infty} \alpha^{1/x} = 1, \quad (24)$$

where α is a constant, it is straightforward to show that by setting $\alpha = N_{\text{init}}$ and solving for $x = m$ Eq. 23 gives

$$\lim_{m \rightarrow \infty} \left(\frac{N_{\text{init}}}{m} \right)^{\frac{1}{m}} = 1 \quad (25)$$

This result has been used to derive Eq. 22 from Eq. 21, see above.

Molecular design principles for predicting self-assembly

The canonical partition function for a system of n molecules at the temperature T and volume V in the limit of idealized highly diluted solutions (i.e. particles can be treated as independent) can be expressed in terms of molecular partition functions as

$$Z(n, V, T) = \frac{[z(V, T)]^n}{n!} \quad (26)$$

By introducing the rigid-rotor harmonic-oscillator approximation (i.e. the rotational and vibrational molecular degrees of freedom can be treated separately) and assuming the independence of the electronic and nuclear degrees of freedom, each molecular partition function can be decomposed as

$$z(V, T) = z_{\text{tr}} z_{\text{rot}} z_{\text{vib}} z_{\text{elec}} z_{\text{nucl}} \quad (27)$$

where z_{tr} , z_{rot} , z_{vib} , z_{elec} , and z_{nucl} are the translational, rotational, vibrational, electronic and nuclear molecular partition functions, respectively. Within these approximations and adopting the convention that $z_{\text{nucl}} = 1$ as done in Ref. [1], the canonical partition function can be finally expressed as

$$Z(n, V, T) = \frac{(z_{\text{tr}} z_{\text{rot}} z_{\text{vib}} z_{\text{elec}})^n}{n!} \quad (28)$$

¹ Assuming that $x = e^{\ln(x)}$ by computing the logarithm at both hand sides one can easily show that $\ln(x) = \ln(e^{\ln(x)}) = \ln(x) \ln(e) = \ln(x)$.

By solving Schrödinger's equation for a particle in a three-dimensional box, a rigid rotor, and a simple harmonic oscillator and evaluating the corresponding partition functions in the classical limit, one can find analytical expressions for the translational,

$$z_{\text{tr}}(V, T) = \left(\frac{2\pi m k T}{h^2} \right)^{3/2} V, \quad (29)$$

the rotational,

$$z_{\text{rot}}(T) = \frac{\sqrt{\pi}}{\sigma} \left(\frac{8\pi^2 I k T}{h^2} \right)^{3/2}, \quad (30)$$

and the vibrational,

$$z_{\text{vib}}(T) = \prod_i^{\kappa} \frac{kT}{h\nu_i}, \quad (31)$$

molecular partition functions, with m the mass, I the moment of inertia, σ the symmetry number, ν_i the frequency of the i -th vibrational degrees of freedom of the molecules. For the sake of rigour we note that: (i) the moment of inertia of an asymmetric top is defined by its principle moments of inertia I_x , I_y , and I_z , such that $I^{3/2}$ in Eq. 30 becomes $(I_x I_y I_z)^{1/2}$; (ii) the symmetry number of a polyatomic molecule is classically introduced to avoid over-counting indistinguishable molecular configurations in phase space and actually corresponds to the number of pure rotational elements (including identity) in the point group of a non linear molecule; (iii) the normal-mode frequencies ν_i in Eq. 31 are wave frequencies, which correspond to $\frac{1}{2\pi} \sqrt{k/\mu}$ for a diatomic molecule having a reduced mass equal to μ and a vibrational constant equal to k . Finally, by neglecting the contributions arising from excited electronic states, which is a good approximation at ordinary temperatures, the electronic molecular partition function can be written as

$$z_{\text{elec}}(T) = \omega_{e1} e^{D_e/kT} \quad (32)$$

with ω_{e1} the degeneracy and $-D_e$ the energy of the ground electronic state; we note that D_e actually corresponds to the energy that is required to break apart the molecule into separated electronically unexcited atoms at rest [1]. Introducing these results into Eq. 27, one can express each molecular partition function in terms of the Physico-Chemical properties of the building blocks for self-assembly as

$$z(V, T) = \left(\frac{2\pi m k T}{h^2} \right)^{3/2} V \cdot \frac{\sqrt{\pi}}{\sigma} \left(\frac{8\pi^2 I k T}{h^2} \right)^{3/2} \cdot \prod_i^{\kappa} \frac{kT}{h\nu_i} \cdot \omega_{e1} e^{D_e/kT} \quad (33)$$

Most importantly, introducing this result into Eq. 26 and using Stirling's approximation we are finally able to express the logarithm of the canonical partition function as a function of the ensemble

conditions (n, V, T) as well as the molecular properties of the building blocks ($m, I, \nu_i, -D_e$)

$$\ln Z(n, V, T) = n \left[\ln \left(\frac{2\pi mkT}{h^2} \right)^{3/2} \frac{Ve}{n} + \ln \frac{\sqrt{\pi}}{\sigma} \left(\frac{8\pi^2 IkT}{h^2} \right)^{3/2} + \sum_i \ln \frac{kT}{h\nu_i} + \ln \omega_{e1} + \frac{D_e}{kT} \right] \quad (34)$$

Indeed, Eq. 34 is key for our theoretical interpretation of self-assembly because, as we shall see, it provides means to translate the three statistical-mechanics principles for predicting self-assembly introduced at the end of *Section 1* (see *Main Text*) into guidelines for chemical design.

Low Initial Entropy

Assuming an idealized solution behavior (i.e. both molecular events and particles can be treated as independent, see *Main Text*), Eq. 34 provides an analytical expression for the absolute entropy,

$$\begin{aligned} S &= \frac{\partial kT \ln Z(n, V, T)}{\partial T} = \\ &= nk \left[\frac{5}{2} + \ln \left(\frac{2\pi mkT}{h^2} \right)^{3/2} + \ln \frac{V}{n} + \right. \\ &\quad \left. \frac{3}{2} + \ln \frac{\sqrt{\pi}}{\sigma} + \ln \left(\frac{8\pi^2 IkT}{h^2} \right)^{3/2} + \sum_i \left(1 + \ln \frac{kT}{h\nu_i} \right) + \ln \omega_{e1} \right], \end{aligned} \quad (35)$$

which can be effectively used to translate the first principle for predicting self-assembly (“Low Initial Entropy”) into chemical words. In fact, Eq. 35 states that any increase in the number of molecules (n) or system’s volume ($\ln V$), as well as in the mass ($\ln m^{3/2}$) or the moment of inertia ($\ln I^{3/2}$) of the molecular building blocks, or equivalently a decrease in their vibrational frequencies ($\ln \frac{kT}{h\nu}$), will lead to an overall increase of the absolute initial entropy. It follows that in order to minimize the initial absolute entropy, so as to cope with the first principle for predicting self-assembly, optimized building blocks should be *light* (low-molecular weight), *isotropic* (symmetric shape) and *stiff* (rigid). Incidentally, we note that within the above approximations it is possible to separate the absolute entropy into three independent contributions such that Eq. 35 can be rewritten as

$$\begin{aligned} S &= S_{\text{tr}} + S_{\text{rot}} + S_{\text{vib}} = \\ &= nk \left[\frac{5}{2} + \ln \left(\frac{2\pi mkT}{h^2} \right)^{3/2} \frac{V}{n} \right]_{\text{tr}} + nk \left[\frac{3}{2} + \ln \frac{\sqrt{\pi}}{\sigma} \left(\frac{8\pi^2 IkT}{h^2} \right)^{3/2} \right]_{\text{rot}} + nk \left[\sum_i \left(1 + \ln \frac{kT}{h\nu_i} \right) \right]_{\text{vib}} \end{aligned} \quad (36)$$

As we shall see, this result is useful to provide a molecular interpretation of the “High Relative Entropy” principle for predicting self-assembly.

Low Final Enthalpy

Starting from the statistical-mechanics definition of the thermodynamic energy in the canonical ensemble,

$$E = kT^2 \frac{\partial \ln Z(n, V, T)}{\partial T}, \quad (37)$$

the result of Eq. 34 can be used to provide a molecular interpretation of the “Low Final Enthalpy” principle for predicting self-assembly. In the limit of idealized solution behavior, in fact, the thermodynamic energy of the assembled state (**b**) is

$$E_b = \frac{3}{2}n_b kT - n_b D_{e,b} \quad (38)$$

that shows that the probability of self-assembly can be increased by increasing $D_{e,b}$, which minimizes the potential energy of self-assembled state (E_b). It is important to note that even small changes in $D_{e,b}$ are expected to produce sizeable effects on the canonical partition function, as the electronic contribution of Eq. 34 is the only term that goes linear with $\ln Z$. In chemical-design words, the optimization required by the “Low Final Enthalpy” principle translates into: (i) maximize the strength of molecular recognition (i.e. the binding energy per building block); and (ii) maximize the coordination number in the final self-assembled state (i.e. the number of nearest neighbors per molecule in the final architecture). The former rule provides guidelines on the type of interactions to be used for predicting self-assembly; the latter conveys information on the structure of the building blocks as well as the topology of the final architecture. In fact, in order to maximize the strength of molecular recognition one should engineer binding sites based on the following interaction types in the given order: covalent bonds (*covalent*) > weak or semi-covalent bonds such as disulfide bridges (*semi-covalent*) > coordinate-covalent bonds in metal-ligand(s) complexes (*metal-ligand*) > charge-charge electrostatic interactions like salt-bridges (*Coulomb*) > H-bonding interactions (*H-bond*) > isotropic Van der Waals interactions (*vdW*). In other words, the “Low Final Enthalpy” principle would prescribe the use of recognition events based on the previous ranking, from the strongest (covalent) to the weakest (vdw), to increase the probability of self-assembly. This conclusion is not very surprising and has been extensively exploited to predict self-assembly of small-molecule compounds. What is perhaps more interesting is that the latter does not hold necessarily true for large molecular building blocks, where the density of interaction sites may play the dominant role. Consistently, the use of vdW interactions, which are individually weak but additive, is common in Nature to promote self-assembly of large biomolecular complexes, such as the virus capsid, where the size of the molecular building blocks and shape

complementarity are likely to be the key to association [2]. In this respect, it is important to note that covalent and semi-covalent interactions, which are expected to contribute significantly to the thermodynamic stability of the assembled state (see above), are perhaps not an optimal choice: on the one hand, they introduce strong constraints on the chemical nature of the building blocks, which dramatically reduce the chemical space available for the molecular design; on the other hand, they strongly reduce the reversibility of the recognition events, which results in high free-energy barriers on the self-assembly pathway and thus frustration. The latter has been recently shown to hamper self-assembly kinetically, making the system behave as a glass at ordinary temperature [3]. By contrast, multiple H-bonding interactions, which can be easily tuned by varying the number of donor and acceptor groups in a single chemical moiety as well as metallo-ligand interactions appear to be the best candidates for predicting self-assembly of medium-sized building blocks.

On the second rule arising from the “Low Final Enthalpy” principle, it is straightforward to see that for a given energy per recognition event, the self-assembled architecture corresponding to the largest number of neighbors (i.e. maximum coordination number) will be thermodynamically most favored. In chemical-design words, the latter implies that molecular scaffolds which are not directly involved in molecular recognition could be engineered as well, for instance to maximize the coordination number (see Fig. S2). Thus, the geometry of the building blocks as well as the number of recognition sites per molecule are expected to play a critical role to program of the final architecture [4].

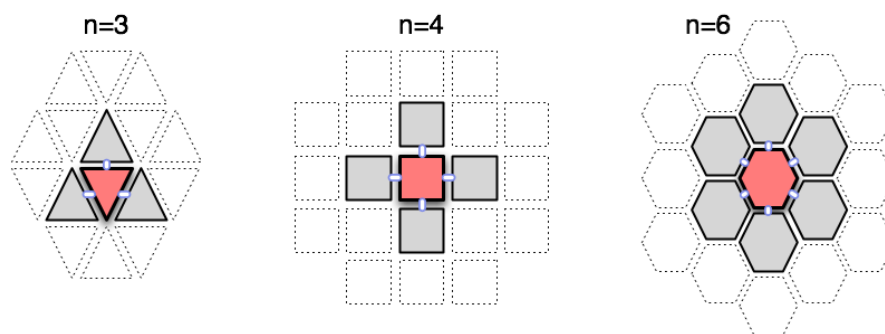


FIG. S2: Engineering supramolecular architectures by modulating the molecular shape and the density of recognition per molecule. Three architecture corresponding to different coordination numbers (n) are shown. Each architecture sketches a typical molecule in the assemble state (red) interacting with n nearest neighbors through recognition events (light blue).

In conclusion, the “Low Final Enthalpy” principle translates into engineering building blocks with strong recognition energies that self-assemble into architectures with high coordination num-

bers. Incidentally, the concurrence of the two would result in molecular building blocks with a strong anisotropy of interactions, which has been recently proposed to be a molecular requirement for the emergence of supramolecular networks at surfaces [5].

High Relative Entropy

Finally, the third principle for predicting self-assembly (“High Relative Entropy”) can be interpreted by analyzing the difference in entropy between the initial disassembled (**a**) and the final self-assembled state (**b**). Specifically, we aim at identifying the molecular determinants that can modulate the entropy change on self-assembly at standard state, i.e. the difference in entropy at chemical equilibrium due to the chemical nature of the species involved.

For the generalized self-assembly reaction, $\alpha a \rightleftharpoons \beta b$, and assuming $\beta = 1$ the entropy change at standard state ² is given by

$$\Delta S_{b,a}^{\circ} = S_b^{\circ} - \alpha S_a^{\circ} \quad (39)$$

By introducing the result of Eq. 36 and rearranging ³, Eq. 39 gives

$$\begin{aligned} \Delta S_{b,a}^{\circ} = & R \left[\ln \left(\frac{m_b}{m_a} \right)^{\frac{3}{2}} - (\alpha - 1) \left(\frac{5}{2} + \ln \left(\frac{2\pi m k T}{h^2} \right)^{\frac{3}{2}} \frac{V}{n} \right) \right]_{\text{tr}} + \\ & R \left[\ln \left[\frac{\sigma_a}{\sigma_b} \frac{\sqrt{I_x I_y I_z}_b}{\sqrt{I_x I_y I_z}_a} \right] - (\alpha - 1) \left(\frac{3}{2} + \ln \frac{\sqrt{\pi}}{\sigma} \left(\frac{8\pi^2 I k T}{h^2} \right)^{\frac{3}{2}} \right) \right]_{\text{rot}} + \\ & R \left[\sum_i^{\alpha(3n_a-6)} \ln \left(\frac{\nu_{i,a}}{\nu_{i,b}} \right) + (\alpha - 1) \sum_i^6 \left(1 + \ln \frac{kT}{h\nu_{i,b}} \right) \right]_{\text{vib}} \end{aligned} \quad (40)$$

where R is the gas constant that replaces nk at standard state. Furthermore, considering that $m_b/m_a = \alpha$, $\sqrt{I_x I_y I_z}_{a,b} = \mathcal{I}_{a,b}^{\frac{3}{2}}$, and $\kappa = \alpha(3n_a - 6)$ (see note ⁴ for details) and using the result of Eq. 36, the entropy change on self-assembly can be meaningfully formulated as

$$\Delta S_{b,a}^{\circ} = R \left(\frac{3}{2} \ln \alpha - (\alpha - 1) S_a^{\text{tr}} \right) + R \left(\frac{3}{2} \ln \frac{\mathcal{I}_b}{\mathcal{I}_a} - (\alpha - 1) S_a^{\text{rot}} \right) + R \left(\sum_i^{\kappa} \ln \left(\frac{\nu_{i,a}}{\nu_{i,b}} \right) + (\alpha - 1) \sum_i^6 S_{i,b}^{\text{vib}} \right) \quad (41)$$

² The standard state is taken to be 1 M, i.e. $n_a = n_b$ and equal to Avogadro’s number, and V is 1 l.

³ The result of Eq. 40 is obtained by considering that $\alpha = (\alpha - 1) + 1$.

⁴ From mass balance the generalized self-assembly reaction $\alpha n_a - \beta n_b = 0$ can be written as $\beta m_b = \alpha m_a$, from which follows that $m_b/m_a = \alpha$ under the assumption that $\beta = 1$. In addition, it is convenient to express the moment of inertia of one particle through the geometric average of its principal components such that $(I_x I_y I_z)_i^{\frac{1}{2}} = \mathcal{I}_i^{\frac{3}{2}}$. Finally, although $N_b = \alpha N_a$, (with N_a and N_b the number of atoms in the monomer and the self-assembled particle, respectively) the actual number of vibrational degrees of freedom varies during association. Thus, a one-to-one comparison of the vibrational frequencies before and after self-assembly can be done only for a reduced number $\kappa = \alpha(3N_a - 6)$ of degrees of freedom.

which provides an expression of the relative entropy on self-assembly in terms of the Physico-Chemical properties of the particles before and after association (m_b/m_a , $\mathcal{I}_b/\mathcal{I}_a$, ν_a/ν_b). Interestingly, Eq. 41 shows that the relative entropy on self-assembly is subjected to three independent contributions, which depend on the *size* (i.e. $\ln \alpha$), the *shape* (i.e. $\ln \frac{\mathcal{I}_b}{\mathcal{I}_a}$), and the *softness* (i.e. $\sum_i \ln \frac{\nu_{i,a}}{\nu_{i,b}}$) of the final self-assembled state. At the same time each component includes a correction which is linear with α and accounts for the stoichiometry of the assembly reaction. Importantly, the stoichiometric-dependent term has a negative sign (i.e. it disfavors association) in the translational and rotational contributions, because it accounts for the loss of three translational and three rotational degrees of freedom per binding event, whereas it has a positive sign (i.e. it favors association) in the vibrational contribution. Overall, Eq. 41 nicely captures the molecular nature of the “High Relative Entropy” principle and can be used to modulate and eventually control the propensity for self-assembly by playing with the chemistry of the building blocks. Illustrative examples on the *size*, the *shape*, and the *softness* dependence of self-assembly are provided below.

Size dependence. The first term of the r.h.s of Eq. 41 corresponds to the translational contribution to the self-assembly entropy change. Its expression,

$$\begin{aligned}\Delta S_{b,a}^{\text{tr}} &= R \left[\frac{3}{2} \ln \alpha - (\alpha - 1) S_a^{\text{tr}} \right] = \\ &= R \left[\frac{3}{2} \ln \alpha - (\alpha - 1) \left(\frac{5}{2} + \ln \left[\left(\frac{2\pi m_a kT}{h^2} \right)^{\frac{3}{2}} \frac{V}{N} \right] \right) \right],\end{aligned}\quad (42)$$

indicates that the difference in translational entropy between the initial disassembled (**a**) and the final self-assembled (**b**) state depends on two contributions of opposite sign: the first is positive and grows logarithmically with α (i.e. the *size* of the supramolecular aggregate); the second is negative and grows linearly with α . According to the “High Relative Entropy” principle the latter disfavors self-assembly and accounts for the loss of three translational degrees of freedom per binding event, S_a^{tr} . As the translational entropy loss is largely dominant, Eq. 42 shows that supramolecular growth into extended architectures is entropically very costly and may be possible only through strong enthalpy/entropy (molecular recognition) or solvent-related entropy/entropy compensations; see Fig. S3. However, it is interesting to note that the translational entropy loss is quite sensitive to the molecular weight of the building blocks, m_a . In fact, Fig. S3 shows that the entropic penalty to form a cluster of 100 model particles decreases by 200 or 400 kcal/mol if m_a is reduced by one or two orders of magnitude. It follows that the molecular mass of the building blocks is a key

parameter that should be carefully considered at the stage of chemical design for self-assembly.

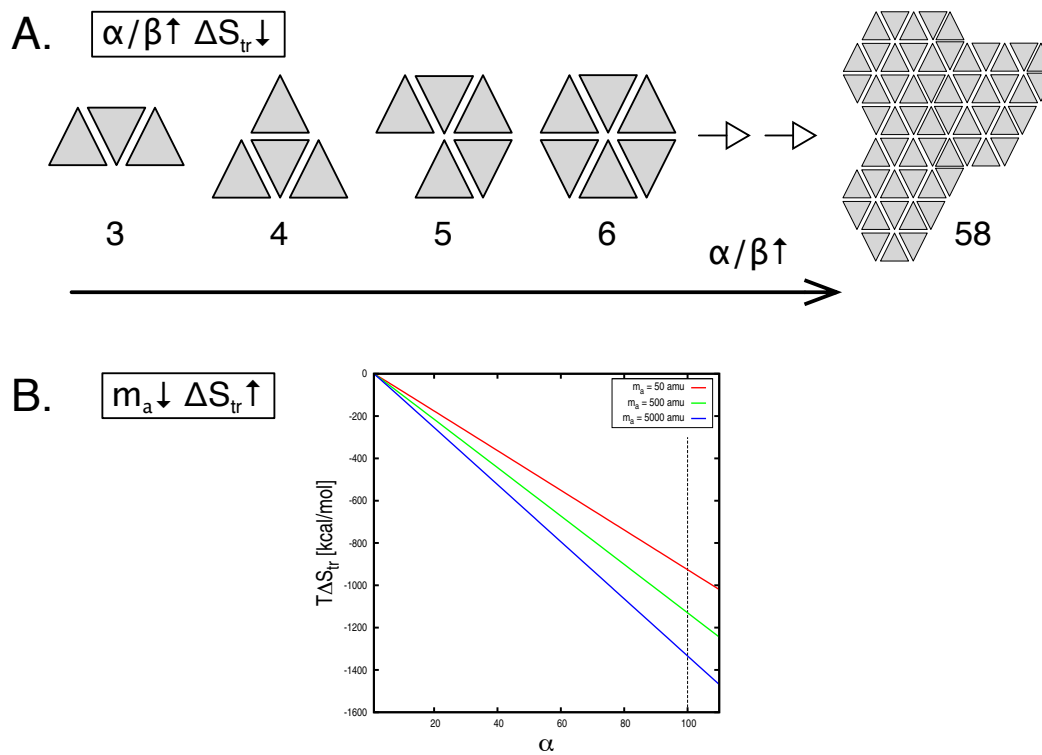


FIG. S3: Size dependence of the entropy change on self-assembly. (A) Supramolecular growth into extended architectures: α and β are the stoichiometric coefficients of the generalized self-assembly reaction, $\alpha a \rightleftharpoons \beta b$; assuming $\beta = 1$, α corresponds to the size of the final supramolecular aggregate. The loss of three translational degrees of freedom per binding event results in a large entropic cost of association, which is linear with α . (B) Entropy change on self-assembly versus the size of the final architecture for three building blocks of increasing molecular weight, m_a . Entropy values were computed at 300 K; they are given in kcal/mol. The data show that the translational entropy cost is strongly dependent on the size of the building blocks.

Shape dependence. The second term of the r.h.s of Eq. 41 corresponds to the rotational contribution to the self-assembly entropy change. Once more its expression,

$$\begin{aligned} \Delta S_{b,a}^{\text{rot}} &= R \left[\frac{3}{2} \ln \frac{\mathcal{I}_b}{\mathcal{I}_a} - (\alpha - 1) S_a^{\text{rot}} \right] = \\ &= R \left[\frac{3}{2} \ln \frac{\mathcal{I}_b}{\mathcal{I}_a} - (\alpha - 1) \left(\frac{3}{2} + \ln \frac{\sqrt{\pi}}{\sigma_a} \left(\frac{8\pi^2 \mathcal{I}_a kT}{h^2} \right)^{\frac{3}{2}} \right) \right], \end{aligned} \quad (43)$$

shows an interplay between two terms of opposite sign: a positive contribution that depends logarithmically on the ratio of the moment of inertia of the assembled architecture over that of the monomeric form and a negative contribution accounting for the loss of three rotational degrees of

freedom per binding event, S_a^{rot} ; we note that the moments of inertia ratio corresponds to the change in particles' *shape* on self-assembly. Interestingly, Eq. 43 provides a quantitative way to access how changes in particles symmetry upon association may affect the self-assembly probability. Starting from a highly symmetric building block, such as C60 fullerene, three supramolecular architectures with different shapes have been modeled by positioning an increasing number of particles on a 1D (linear), 2D (square), or 3D (cubic) regular lattice. The rotational entropy change on self-assembly were then predicted for each architecture by using Eq. 43 for increasing α ; see Fig.S4. The data show that despite a sizeable change in the moment of inertia of the final architecture, \mathcal{I}_b , the shape-dependent contribution is negligible with respect to the rotational entropy loss, which indeed governs the rotational contribution. In close analogy to the translational entropy (see above), the rotational entropy loss on association appears to be so sensitive to changes in *shape* of the building blocks, that the corresponding entropic cost to form a cluster of about 100 molecules may be reduced by 70 or 140 kcal/mol by decreasing by one or two orders of magnitude the moment of inertia of monomeric particles, \mathcal{I}_a . We conclude that the *shape* (or the symmetry) of the building blocks is another key factor that should be optimized at the stage of chemical design for self-assembly.

Softness dependence. The last term of the r.h.s of Eq. 41 corresponds to the vibrational entropy contribution,

$$\begin{aligned} \Delta S_{b,a}^{\text{vib}} &= R \left[\sum_i^{\kappa} \ln \left(\frac{\nu_{i,a}}{\nu_{i,b}} \right) + (\alpha - 1) \sum_i^6 S_{i,b}^{\text{vib}} \right] = \\ &= R \left[\sum_i^{\kappa} \ln \left(\frac{\nu_{i,a}}{\nu_{i,b}} \right) + (\alpha - 1) \sum_i^6 \ln \left(1 + \frac{kT}{h\nu_{i,b}} \right) \right], \end{aligned} \quad (44)$$

which depends logarithmically on the inverse ratio of the vibrational frequencies of the final self-assembled architecture over those of the initial monomeric particles. Interestingly and in sharp contrast to the translational and rotational components, Eq. 44 includes a term linear with α with a positive sign. The latter implies that self-assembly does not necessarily involve a vibrational entropy loss, as the sign of the overall $\Delta S_{b,a}^{\text{vib}}$ will depend on the inverse ratio of the vibrational frequencies. In fact, if $\frac{\nu_{i,a}}{\nu_{i,b}}$ is on average larger than zero (i.e. monomers are more rigid than the self-assembled architecture), its logarithm will be positive and the vibrational entropy contribution will favor self-assembly; if not, $\Delta S_{b,a}^{\text{vib}}$ will be negative and disfavor self-assembly. Interestingly, Eq. 44 indicates that if we are able to arrange objects in space in such a way that the resulting architecture is much "softer" than the individual monomers (i.e. it vibrates at lower frequencies),

self-assembly may be entropically driven [6]. Thus, given a set of n self-assembly particles the “softest” arrangement, i.e. the one that minimizes the overall vibrational frequencies, will have the largest vibrational entropy stabilization. Clearly, the latter depends on the *topology*, and thus the *shape* of the self-assembled architecture, and the nature of the interactions among particles (i.e. their strength, directionality, short- or long-range character, etc.). In the limit of the above approximations, Eq. 44 captures all these aspects and allows to translate them into chemical-design rules. In fact, in the range of validity of the harmonic approximation one may determine the particles’ vibrational frequencies before and after association by normal-mode analysis and estimate the vibrational entropy change on self-assembly by using Eq. 44. To illustrate the dependence of the vibrational entropy contribution on the topology of the self-assembled architecture, the size of $\Delta S_{b,a}^{\text{vib}}$ was investigated for a series of two-dimensional discrete objects (i.e. molecular cycles) as a function of α ; see Fig. S5. The results are given in Table S1. The data show that the low-frequency modes of the assembled particles (i.e. their global motions) strongly depend on the size of the aggregate. Indeed, the lowest frequency mode decreases from 44 to 10 cm^{-1} on going from the dimer to a 15-mer. Effectively, this corresponds to a non-negligible entropic stabilization of the assembled state, which is quantified to be roughly 20 kcal/mol at room temperature for our model system. Thus, playing with the topology of the resulting architecture, as well as the strength of the interaction between particles appear as a promising route to control molecular self-assembly. By extrapolating these results, we expect sizeable entropic stabilizations for large supramolecular objects such as mesoscale soft-materials (see *Section 2*) or crystalline architectures (see *Section 3*).

n_b	1	2	3	5	10	15
lowest ν [cm^{-1}]	/	44.3	38.3	36.8	19.4	9.8
$\Delta S_{b,a}^\circ$ [e.u.]	/	5.06	15.4	25.4	52.9	63.5
$T\Delta S_{b,a}^\circ$ [kcal/mol] (@ 300K)	/	1.5	4.6	7.6	15.9	19.1

TABLE S1: Softness dependence of the relative entropy for self-assembly at standard state evaluated for the series cyclic aggregates depicted in Fig. S5. n_b is the number of building blocks per object. Objects were constructed assuming a regular polygonal topology, setting the inter-particle distance at 1.5 Å and connecting particles by harmonic springs with a force constant of 1 kcal/mol/Å². Frequencies were determined by diagonalizing the Hessian Matrix obtained in the elastic network approximation [7]. Relative vibrational entropy values for the various aggregates are given both in entropy units (e.u) and kcal/mol at room temperature (i.e. 300 K).

Entropy loss upon confinement at the solid-liquid interface

The translational partition function per molecule in n dimensions [1] is

$$z_{\text{tr}} = \left(\frac{2\pi mkT}{h^2} \right)^{n/2} a^n \quad (45)$$

with m the mass, k the Boltzmann constant, h the Plank constant, and a^n the generalized volume.

For N non-interacting molecules the system's translational partition function is

$$\begin{aligned} Z_{\text{tr}} &= \frac{z_{\text{tr}}^N}{N!} \\ \ln Z_{\text{tr}} &= N(\ln z_{\text{tr}} - \ln N + 1) \end{aligned} \quad (46)$$

By using the result of Eq. 29, the latter becomes

$$\ln Z_{\text{tr}} = N \left[\frac{n}{2} \ln \left(\frac{2\pi mkT}{h^2} \right) + \ln \frac{a^n e}{N} \right] \quad (47)$$

As the free energy is defined as

$$F = -kT \ln Z, \quad (48)$$

the translational free energy for a system of N molecules in n dimensions is

$$F_{\text{tr}}^n = -NkT \left[\frac{n}{2} \ln \left(\frac{2\pi mkT}{h^2} \right) + \ln \frac{a^n e}{N} \right] \quad (49)$$

It follows that the free energy cost of confining N molecules in solution (i.e. 3D) to a layer at the solid-liquid interface (i.e. 2D) equals

$$\Delta F_{3D \rightarrow 2D} = F_{\text{tr}}^2 - F_{\text{tr}}^3 = NkT \left[\frac{1}{2} \ln \left(\frac{2\pi mkT}{h^2} \right) + \ln a \right] \quad (50)$$

which for a number of Avogadro (N_a) molecules becomes

$$\Delta F_{3D \rightarrow 2D} = RT \left[\frac{1}{2} \ln \left(\frac{2\pi mkT}{h^2} \right) + \ln a \right] \quad (51)$$

We note that the second term of the r.h.s. of Eq. 51 depends on the system's volume (i.e. a^3) and thus on the initial concentration. At standard conditions, i.e. 1M concentration, the volume is 10^{-3}m^3 such that a is 10^{-1} m. By using an arbitrary molecular mass of 500 gram/mol (i.e. $m = 8.30269e-25$ Kg), a temperature of 300 K, $k = 1.3806504e-23$ J/K, $h = 6.62606896e-34$ Js, Eq. 51 yields a free energy cost of 14.2 kcal/mol.

[1] D. McQuarrie, Statistical Mechanics, New York: Harper and Row, 1976.

- [2] A. Olson, Y. Hu, E. Keinan, Chemical mimicry of viral capsid self-assembly, *Proceedings of the National Academy of Sciences* 104 (52) (2007) 20731.
- [3] C. Palma, P. Samor, M. Cecchini, Atomistic Simulations of 2D Bicomponent Self-Assembly: From Molecular Recognition to Self-Healing, *Journal of the American Chemical Society* (2010) 1312.
- [4] A. Ciesielski, A. Cadeddu, C. Palma, A. Gorczyński, V. Patroniak, M. Cecchini, P. Samorì, Self-templating 2d supramolecular networks: a new avenue to reach control over a bilayer formation, *Nanoscale*.
- [5] U. Weber, V. Burlakov, L. Perdigao, R. Fawcett, P. Beton, N. Champness, J. Jefferson, G. Briggs, D. Pettifor, Role of interaction anisotropy in the formation and stability of molecular templates, *Physical review letters* 100 (15) (2008) 156101.
- [6] A. Cooper, D. Dryden, Allostery without conformational change, *European Biophysics Journal* 11 (2) (1984) 103–109.
- [7] M. M. Tirion, Large amplitude elastic motions in proteins from a single-parameter, atomic analysis 77 (1996) 1905–1908.

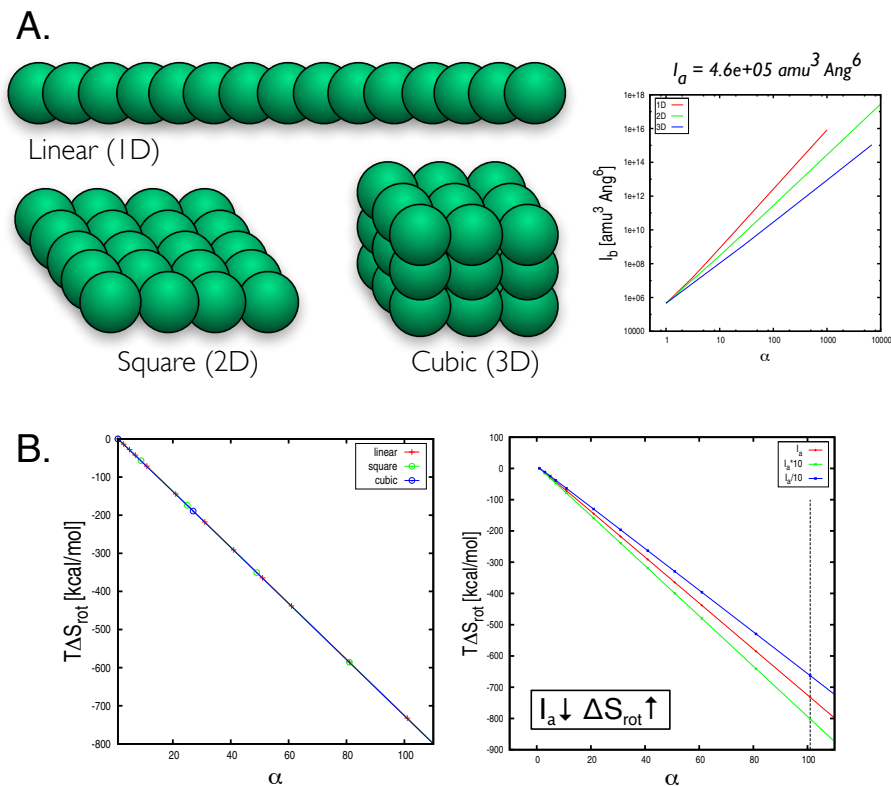


FIG. S4: Shape dependence of the entropy change on self-assembly. (A) Dependence of the moment of inertia of the assembled architecture (I_b) on the *size* and the *shape*. Three different architectures were analyzed; they were modeled by positioning an increasing number of C60 fullerene particles onto a 1D (linear), 2D (square), or 3D (cubic) regular lattices. The moment of inertia of each building block was $I_a = 4.6 \cdot 10^5 \text{ amu}^3 \text{ \AA}^6$. On the right-hand side, the data show that I_b is strongly dependent on the *shape* of the molecular aggregate; i.e. for an aggregate of about 100 molecules it increases by one or two orders of magnitude on going from the cubic to the linear arrangement. (B) Rotational entropy loss on self-assembly. Relative entropy values at 300 K are given in kcal/mol. On the left-hand side, the rotational entropy contribution at room temperature is reported for the three architectures as a function of α (i.e. the *size* of the supramolecular aggregate). The data show that despite the strong shape-dependence of the moment of inertia (see above), the shape-dependent entropic contribution is negligible with respect to the rotational entropy loss upon association. On the right-hand side, the rotational entropy contribution for increasing α is given for three monomers of varying I_a . The data show that the rotational entropy loss is highly sensitive to changes in the *shape* of the building blocks, such that a reduction of I_a by one or two orders of magnitude corresponds to a decrease of 70 to 140 kcal/mol for a cluster of 100 molecules.

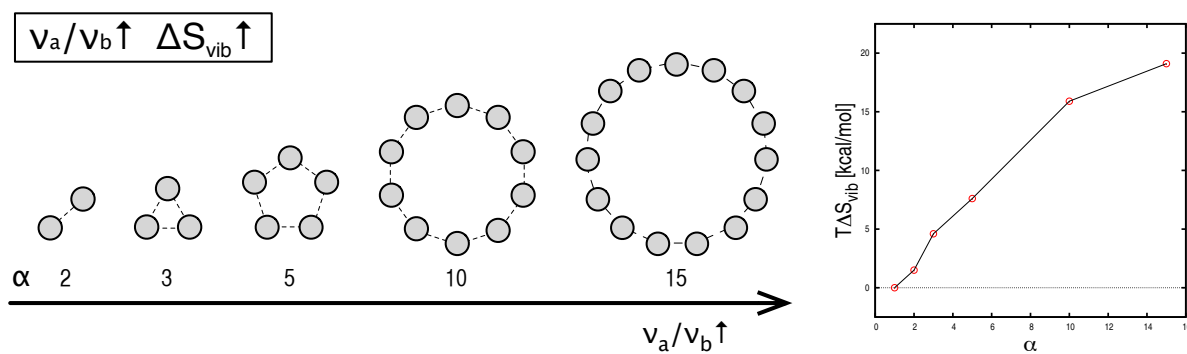


FIG. S5: Softness dependence of the entropy change on self-assembly. The vibrational entropy change of a series 2D discrete model architectures is analyzed as a function of α , i.e. the size of the molecular aggregate. For simplicity, objects were modeled as regular polygons made by particles connected with springs of equal strength. The distance between particles was chosen to be 1.5 \AA and springs were modeled using a harmonic strength of 1 kcal/mol/\AA^2 , which roughly mimics the recognition strength provided by non-covalent interactions such as H-bonding. On the right-hand side, it is shown that the vibrational entropy stabilization for a 15-mer cycle at room temperature can be as large as 20 kcal/mol .